Holoprosencephaly and Cyclopia in *bmp7b* and *bmpr1ba* Crispant zebrafish

Valentyn Kyrychenko[1], Philipp Rensinghoff[1], Johannes Bulk[1], Constanze Frey[1] and Stephan Heermann[1,2]

[1] Department of Molecular Embryology, Institute of Anatomy and Cell Biology, Faculty of Medicine, University Freiburg, 79104 Freiburg, Germany
[2] Faculty of Health, Security, Society, Furtwangen University, Furtwangen, Germany

Corresponding author: Stephan.heermann@hs-furtwangen.de

Abstract

The visual system is highly specialized and its function is substantially depending on the proper development of the eyes. Early eye development starts with the definition of a single eye field, which is localized within the anterior neural plate (ANP). This single eye field is split consecutively and two optic vesicles emerge at the sides. These vesicles are then transformed into optic cups, out of which the future retinae are differentiating.
Holoprosencephaly (HPE) is a frequent developmental forebrain disorder, in which the splitting of ANP domains is hampered. HPE is mostly genetically linked and we recently showed that BMP antagonism is important for the eye field and the telencephalic anlage to split. Excessive BMP induction led to retinal progenitors stuck inside a dysmorphic forebrain.
In this study, using the zebrafish as a model, we show with acute CRISPR/ Cas9 analysis in the F0 generation, the necessity of *bmp7b* and *bmpr1ba* for proper forebrain development. In Crispants for both genes we found HPE phenotypes, e.g. cyclopia. Further analysis of *bmp7b* Crispants indicated that predominantly the eye field is affected, rather than the telencephalic precursor domain.

Key words: *bmp7b*, *bmpr1ba*, holoprosencephaly, cyclopia, BMP

Introduction:

The development of the nervous system and especially the development of the brain is a fascinating yet intricate process. Most of the bilateral elements of the central nervous system, importantly the telencephalic lobes and the two retinae, are derived from respective single precursor domains which are split during consecutive stages of development.
It has been shown that BMP antagonists are among other factors important for the induction of pre-neural identity within the future neural plate, while BMP signaling activity is rather inducing epidermal fate (Thawani and Groves, 2020; Wilson and Edlund, 2001).
Slightly later within the Anterior Neural Plate (ANP) the prospective eye field and the prospective forebrain are competing with each other and BMP signaling is important to promote telencephalic fate at the expense of eye field fates (Bielen and Houart, 2012).
We showed recently that during consecutive stages of development BMP antagonism is important for the proper separation of the telencephalic precursor domain, eye field splitting and the initial out-pocketing of the optic vesicle from the forebrain (Bulk et al., 2023). Induced expression of *bmp4* (8.5 hpf) resulted in anophthalmic embryos, yet showing retinal progenitors stuck inside a dysmorphic forebrain, a crypt-oculoid. These embryos were not merely ventralized as resulting from a zygotic injection of BMP ligand RNA, e.g. *bmp7a/b* (Bongiovanni et al., 2024; Willot et al., 2002). Though, early axis formation in vertebrates is strongly influenced by BMP ligands (ventral fates) and BMP antagonists (dorsal fates) organized in gradients (Pomreinke et al., 2017). Knock down of BMP antagonists in zebrafish result mostly in a ventralization of the embryo (Dasgupta et al., 2021). In some cases a Knock down can, however, also result in a dorsalization of the embryo, e.g. *tsg* (Little and Mullins, 2004). In mouse, a double Knock Out of two antagonists, Noggin and Chordin, resulted in variably affected morphogenesis of the head and importantly the forebrain but also in cases of cyclopia (Bachiller et al., 2000). In chicken, Holoprosencephaly (HPE) and cyclopia but not anophthalmia were reported after BMP soaked bead implantation (Bmp4 and Bmp5) into the developing ventral telencephalic region (Golden et al., 1999).
In a previous analysis of our group, studying the role of BMP signaling for retinotectal projections, we found that *bmp7b* as well as specific BMP receptors (e.g. *bmpr1ba*) were transcriptionally repressed upon *bmp4* induction (induction at 15 hpf analysis at 21 hpf) (Knickmeyer et al., 2021). This was raising the question, whether a repression of e.g. *bmp7b* could be involved in the formation of the phenotypes resulting from *bmp4* induction, e.g. HPE, morphogenetic defects during optic cup and optic fissure formation with coloboma.

Several Bmp7 mouse Knock Outs resulted in microphthalmia or anophthalmia or affected the formation of the optic fissure (Dudley et al., 1995; Karsenty et al., 1996; Luo et al., 1995; Morcillo et al., 2006; Wawersik et al., 1999a). In zebrafish two *bmp7* paralogous genes were identified. The gene originally termed *bmp7* (the mutant for this is snailhouse, *snh*) is now termed *bmp7a.* In *snh* mutants a mild microphthalmia was described (Willot et al., 2002). The more recently identified paralog is termed *bmp7b* (Shawi and Serluca, 2008). The paralog *bmp7b* is showing a closer homology to human and mouse Bmp7 (Shawi and Serluca, 2008). We, thus became interested in the relation of BMP antagonism/*bmp4* induction and loss of *bmp7b*.
Besides the *snh* mutant, two CRISPR/Cas induced mutants for both paralogs have been established recently (Dong et al., 2022). Notably, while *bmp7a* mutants died during gastrulation, no strong effect regarding eye development could be observed in *bmp7b* mutants.

Before, also our group targeted the *bmp7b* locus in zebrafish with the aim to generate a mutant line and heterozygous fish were raised. To our surprise, in homozygous in-crossed embryos, however, we could not observe an affected development, other than a mild delay in pigmentation (unpublished). Assuming that genetic compensation (El-Brolosy and Stainier, 2017; El-Brolosy et al., 2019) was preventing stronger phenotypes, this approach was not followed further.
In this study, we instead aimed for an acute targeting strategy of the *bmp7b* locus and the *bmpr1ba* locus and an analysis in F0. We found severe forebrain and ocular phenotypes e.g. cyclopia in F0 crispants for *bmp7b* and *bmpr1ba*. The phenotypes were highly reproducible. Further analysis of the ANP in crispants for *bmp7b* showed a dysregulation of markers for the prospective telencephalic domain and eye field.

Results:

Expression domains of BMP ligands and receptors
We addressed the expression of BMP ligands and BMP receptors with wmish at 11 hpf in lateral and dorsal views in wildtype zebrafish (**Figure 1 A-F', G-M' showing schematic representations**). We found ligands and receptors expressed within the ANP, like *bmp7b* (**Figure 1 C and C')** and *bmpr1ba* (**Figure 1 E and E')** and *bmpr1aa* (**Figure 1 D and D')**, or adjacent to the ANP, like *bmp4* (**Figure 1 A and A')**, *bmp7a* (**Figure 1 B and B')** and *bmpr2b* (**Figure 1 F and F')**.

Loss of *bmp7b* and *bmpr1ba* results in eye developmental defects and HPE
We next targeted the zebrafish *bmp7b* locus with Crispr/Cas9. Experimental details, please find in the Materials and Methods section. We injected sgRNAs and RNA for Cas9 into zebrafish zygotes and addressed the phenotypic outcome at 48 hpf (**Figure 2A, scheme**). A spectrum of eye developmental defects was visible ranging from ocular hypotelorism over synophthalmia to cyclopia (**Figure 2C, A shows a wt, Figure 2 Supplement**). In a few cases also anophthalmia occurred. Phenotypes were highly reproducible.
In Morphants for *bmp7b*, addressed before, only a mild ocular hypotelorism and morphogenetic coloboma were found (**not shown**).

We next addressed the zebrafish *bmpr1ba* locus with Crispr/Cas9. For experimental details please visit the Materials and Methods section. Crispr/Cas cocktails were injected into zebrafish zygotes and phenotypes were addressed at 48 hpf. Similar phenotypes regarding the eyes were observed including microphthalmia, anopththalmia, coloboma, synophthalmia and importantly as well as cyclopia (**Figure 2D, A shows a wt, Figure 2 Supplement**).

The efficiency of induction of cyclopia was higher in the cases in which *bmp7b* was targeted (**Figure 2 E, F**). We thus aimed to make use of this approach for further analysis of ANP development.

Loss of *bmp7b* affects eye field splitting
We next aimed to investigate how the loss of *bmp7b* affects the development of the anterior neural plate (ANP). Even though the induced phenotypes, like cyclopia, were highly reproducible, the efficiency observed after injections was yet quite low in the F0 generation.

In humans, HPE is very often lethal at embryonic stages (Matsunaga and Shiota, 1977). Thus, we reasoned that for our experimental paradigm high rates of embryonic lethality resulting from our Crispr/Cas9 injections were acceptable. Our primary aim was to achieve a high level of HPE phenotypes in potentially surviving embryos. To this end, we increased the Crispr/Cas9/ sgRNA dosages (*bmp7b*) (**Figure 2 G)**. This adaption resulted in fewer to zero surviving embryos, however, enabled us to address ANP development in F0 embryos (**Figure 3, scheme of experimental design**).

We used the following paradigm for the analyses (**Figure 3, scheme of experimental design**). In brief, we injected the sgRNAs and Cas9 RNA into zygotes and separated the injected embryos at 11 hpf into two groups. Un-injected embryos of the clutches served as controls to record the injection-independent death rate. One group of injected embryos was fixed and processed for wmish. The other group of injected embryos was grown until 48 hpf to 72 hpf in order to assess the efficiency of the respective injections, giving us an estimate of the percentage of phenotypes which were to be expected also in the fixed embryos of the respective experiment**.**

Next, we addressed the expression of genes, functioning as markers for domains of the ANP. To this end we performed wmish using the embryos of the first group, fixed and processed at 11 hpf (**Figure 3, scheme**). During analysis of the effect of targeting the *bmp7b* locus, we noticed that some genes were reduced in expression, although the expression domain of these genes was relatively normal, if the genes were found expressed. This was the case for genes expressed within the prospective telencephalic domain, *emx3* and *foxg1a* (**Figure 3 A-H**). Genes expressed within the eye field, *six3b*, *rx3* and *cxcr4a* (**Figure 3 I-T)**, however, showed an altered expression domain, which was found more condensed to the midline (**Figure 3 J, N, R)**. Overall, our data show a clear defect in the process of eye field splitting, while a splitting defect of the prospective telencephalic domain could not be shown.

Expression of a*lcamb* was found largely reduced (**Figure 4 A-D**), while the expression of *zic2a* was also found altered, with an extended width in between the lateral expression domains and reduced expression in the transverse domain in the posterior ANP (**Figure 4 E-H**).

Expression domain of *bmpr1ba* is affected by induced levels of *bmp4*

We next asked whether the expression of our current target genes, *bmp7b* and *bmpr1ba*, is affected by early induced levels of *bmp4*, oversaturating endogenous BMP antagonists and resulting in anophthalmic holoprosencephaly (Bulk et al., 2023). To address this, we made use of an established transgenic line, which is expressing *bmp4* upon a heat-shock (Bulk et al., 2023; Knickmeyer et al., 2018). We performed heat-shocks at 8.5 hpf and processed the embryos for wmish at 11 hpf (**Figure 5 scheme)**. The expression of *cmlc2:GFP* (bleeding heart, BH) was not yet active at 11 hpf. Thus, wmish were performed with subsequent genotyping. The expression intensity as well as the expression domain of *bmp7b* was not altered upon an induction of *bmp4* (**Figure 5 C, C' and A, A' as control**). However, the expression domain of *bmpr1ba* was changed (**Figure 5 D, D' and B, B' as control**). The expression domain in wildtype embryos was split into an anterior and a posterior domain (**Figure 5 B, B').** The domain showing reduced to absent levels of expression was the prospective hypothalamic domain, in between the ANP and the midbrain-hindbrain region, both expressing *bmpr1ba* (**Figure 5 B, B'**). The induction of *bmp4*, however, resulted in a

more continuous expression of *bmpr1ba*, potentially at a slightly reduced level, but showing an enhanced level in the prospective hypothalamic domain (**Figure 5 D, D'**).
We next asked whether the few embryos which presented an anophthalmia phenotype in our current study, would also show a crypt oculoid, expressing *rx2*, as we found resulting from inductions of *bmp4* previously (Bulk et al., 2023). To this end we addressed the expression of *rx2* in a few of these embryos. We did not find rx2 expressing oculoids in these anopththalmic embryos (**Figure 5 supplement)**.

Summary/Discussion/Outlook:
During early forebrain development the single prosencephalic domain, containing the presumptive telencephalon, eye-field and hypothalamus, must be split. Pathologies during this event result in a forebrain disorder, termed holoprosencephaly (HPE) for which various genetic factors and also some environmental risk factors have been described (Addissie et al., 2021; Tekendo-Ngongang et al., 1993). As to be expected the clinical manifestation is variable in severity also showing a spectrum of ocular phenotypes (Pineda-Alvarez et al., 2011). We became interested in these ocular phenotypes. We found that BMP antagonism, is crucial for proper optic vesicle to optic cup transformation (Heermann et al., 2015) and also for the preceding initial optic vesicle splitting and out-pocketing (Bulk et al., 2023) both being prevented by experimental induction of *bmp4*. This was providing a reasonable link between morphogenetic coloboma and anophthalmia, both associated with HPE. In the current analysis we targeted the zebrafish loci for *bmp7b* and *bmpr1ba*, two genes, which we found to be transcriptionally regulated by induction of *bmp4* in a different and developmentally later context (Knickmeyer et al., 2021).
We aimed at generating a Crispr induced mutant zebrafish line for *bmp7b* earlier, which was unsuccessful insofar only a delayed pigmentation could be observed in our mutants. We mistrusted these data, because strong phenoptypes were found in bmp7 KO mice and we observed phenotypes in morphants for *bmp7b* even earlier (not shown). Becoming aware of genetic compensation mechanisms (El-Brolosy and Stainier, 2017; El-Brolosy et al., 2019), potentially obscuring phenotypes, and the possibility to address reverse genetics even in the F0 generation (Wu et al., 2018), we restarted our efforts aiming for analyses in F0. Later, we noticed that also others were targeting *bmp7b* in zebrafish to establish a mutant line (Dong et al., 2022). These authors observed defects in eye-development e.g. enlarged iris and increased thickness of the retinal pigment layer (Dong et al., 2022). Importantly they also showed that the RNA for *bmp7b* was still found in their mutants. Such persisting transcription and RNA production is part of the well described genetic compensation mechanism (El-Brolosy et al., 2019), which could also be obscuring stronger phenotypes in the mutants generated by Dong and colleagues.
In this study we targeted the zebrafish loci acutely to address potential phenotypes in the F0 generation. After observing strong HPE phenotypes reproducibly, we aimed to increase the efficiency of our targeting procedure. We were lucky to be provided with genetically enhanced versions of CAS9 mRNA by dear colleagues (Thumberger et al., 2022), enabling us to achieve high targeting efficiencies. These high efficiencies, observed in the few surviving embryos of the second group of injected clutches, were of utmost importance to enable the discovery differences in the expression of genes at embryonic stages (11 hpf) in which the phenotype in the Crispants was not yet visible by pure observation. We reasoned this to be good approach since also in humans affected by HPE embryonic lethality is very high. Even though the incidence in live births is approximately 1/10000 the estimated incidence per

conception is as much as 0.4 % determined in abortions in the 60s and 70s (Matsunaga and Shiota, 1977).

Our key finding in this study is cyclopia and a spectrum of milder effects, e.g. synophthalmia, which is to be expected since the analysis in the F0 generation needs individual targeting events in every single embryo, which surely goes along with a variable efficiency. We observed similar phenotypes including cyclopia in Crispants for both *bmp7b* and *bmpr1ba*, suggesting that for eye field splitting both are essential and bmp7 is acting via bmpr1ba. Naturally, also a bmpr type II must be involved, however, this was not further addressed by this study.

We also observed few cases of anophthalmia. There we did not find *rx2* expressing crypt-oculoids as we found in HPE and anophthalmia regularly resulting from experimental induction of *bmp4*. This suggests a different underlying pathology in these different forms of anophthalmia, which we did not follow up any further.
Otherwise, the induction of *bmp4* was affecting at least the expression of *bmpr1ba*. We observed an enhanced expression in the hypothalamic domain in induced embryos. In wildtypes this domain was largely lacking expression of *bmpr1ba*. It is conceivable that the eye-field splitting defect observed upon *bmp4* induction (Bulk et al., 2023) could be functionally involving also bmp7/bmpr1ba, even though the final outcome is differing and presenting anophthalmia instead of cyclopia.
In our current study we addressed ANP domains and how they were affected by targeting *bmp7b*. With huge experimental effort, we discovered that in Crispants for *bmp7b* the precursors of the eye-field were not separated properly while no clear defect in the division of the telencephalic domain was found (**Figure 6 summary**). The latter is in contrast to the phenotypes derived from *bmp4* induction, in which precursors of both eye-field and telencephalic domain were affected and remaining condensed to the midline. Another interesting difference is the control of the early eye-field gene *rx3*, which is virtually absent after induction of *bmp4* and condensed to the midline in *bmp7b* Crispants. These difference in domain-behavior and gene expression and phenotypic outcome might add to explain the different ocular phenotypes associated with HPE eventually. Nonetheless, at the current stage it is not yet clear whether or not these aspects are linked.
What seems to be obvious, otherwise, is that during forebrain development the ligands bmp4 and bmp7b are acting differentially. Induction of *bmp4* and Crispant for *bmp7b*, both result in HPE. This is not quite surprising on the other hand, since it is long been clear that different bmp ligand subfamilies according to phylogenetic relationships and sequence similarity make use of specific receptor assemblies and besides due to different biochemical properties for instance also show different interaction with matrix components (Gipson et al., 2020).

We make use of the zebrafish model system to learn more about brain and eye development of the human being. Of course, the basics of vertebrate development are conserved, making zebrafish a very powerful model. Nonetheless, there are differences, one of which is the additional genome duplication in teleosts, which did not occur in human or mice. In mice for instance, one gene for bmp7 exists, in zebrafish on the other hand, there are two. In mouse Knock Outs for Bmp7 result in ocular phenotypes (Dudley et al., 1995; Morcillo et al., 2006; Wawersik et al., 1999b) ranging from failures of optic fissure formation to anophthalmia.

In zebrafish the paralogous gene *bmp7b* is considered the closer homolog to the murine bmp7.
It is not clear to us why in zebrafish we find HPE with cyclopia predominantly, while in mouse loss of BMP7 is associated with anophthalmia.

Overall, with this study we provide novel insights for the development of the forebrain and the related pathology HPE. Besides, we provide the community with another experimental model for induces HPE. The new insights found in our study, however, have also raised new questions, which will need further analyses.

Materials and Methods:

Zebrafish care
Zebrafish were housed in accordance with the local animal welfare law and with the following permit from the "Regierungspräsidium Freiburg": 35-9185.64/1.1. The fish were maintained at 28°C in a 12h light/ 12h dark cycle in a recirculating system. The following transgenic line was used: *tg(hsp70l:bmp4, myl7:eGFP)*(Knickmeyer et al., 2018). The zebrafish embryos were grown in petri dishes containing zebrafish medium, 0.3g/l sea salt in deionized water.

Heat shock procedures
For application of a heat-shock for induction of inducible transgenes, embryos were incubated in 1.5 ml reaction tubes at 37°C (heating block, Eppendorf Thermomixer). The onset of the heat shock was 8.5 hpf and the duration was 15 minutes.

Image Processing
Images recorded by microscopy (Nikon, binocular) were edited consecutively for presentation via Inkscape (Inkscape Project. (2020). *Inkscape*. Retrieved from https://inkscape.org).

In situ hybridization
Whole-mount ISHs (wmishs) were performed as described previously (Bulk et al., 2023; Quiring et al., 2004). Probes were partially designed cloning free (Hua et al., 2018).
The following probes were used: *bmp4* (Knickmeyer et al., 2018b), *bmp7a* (F: GCAGCGGGAAATCCTCTCTA, R: GCTTCGGGACAGTTTCAGGG), *bmp7b* (F: GAGACGAAGAGGGCTTCTCG, R: CAGGATGACGTTGGAGCTGT), *bmpr1aa* (F: TAGCCAACCCCAATGCTTAC, R: TAATACGACTCACTATAGGGCCCATTTGTCTCGCAGGTAT (Alexander et al., 2014)), *bmpr1ba* (F: AGAATCTCTGCGGGATCTCA, R: GCTCCGTTTCTCTTGACCAG (Alexander et al., 2014)), *bmpr2b* (F: TATTGTCGCGCTGTTCTTTG, R: GCAGATAGGCCAGTCCTCTG (Alexander et al., 2014)), *cxcr4a* (F: TGGGTTGCCAGAAGAAATCC, R: CCAGAAAGGCGTACAGGATC), *alcamb* (F: CACCCTCTCGCTACAACTTC, R: CTTCTTGCTCTCCTCTGCTG), probes for *emx3*, *foxg1a*, *six3b*, *rx3*, *zic2a*, *rx2* were previously used (Bulk et al., 2023).

CRISPR/Cas9 F0 analysis (Crispants)

Fertilized eggs (1-cell stage embryos) were microinjected with a cocktail of Cas9 mRNA (Thumberger et al., 2022) and sgRNAs for *bmp7b* or *bmpr1ba* respectively. sgRNAs were designed using CCTop (http://crispr.cos.uni-heidelberg.de) (Stemmer et al., 2015).
For *bmpr1ba* the following sgRNAs (sequences: T1: CCGTTACGCACACCTAGTGA and T2: CAGGGAACTCCAAGCAGCGG) were used with a concentration each 15 ng/µl in combination with 150 ng/µl Cas9 mRNA.
For *bmp7b* the following sgRNAs (T1: CAATCCTCGGGTTACCGCAC, T4: TCTATACTCGCGATCCTCCG) were used with a concentration each 30 ng/µl in combination with 150 ng/µl Cas9 mRNA.

Acknowledgements

We thank all members of the Heermann lab for insightful discussions and Ute Baur for great technical assistance. We want to thank Eleni Roussa and Klaus Unsicker for support of the Heermann lab. We also want to thank Jochen Wittbrodt and Thomas Thumberger for providing new and enhanced versions of the CAS9.

Figures and Legends

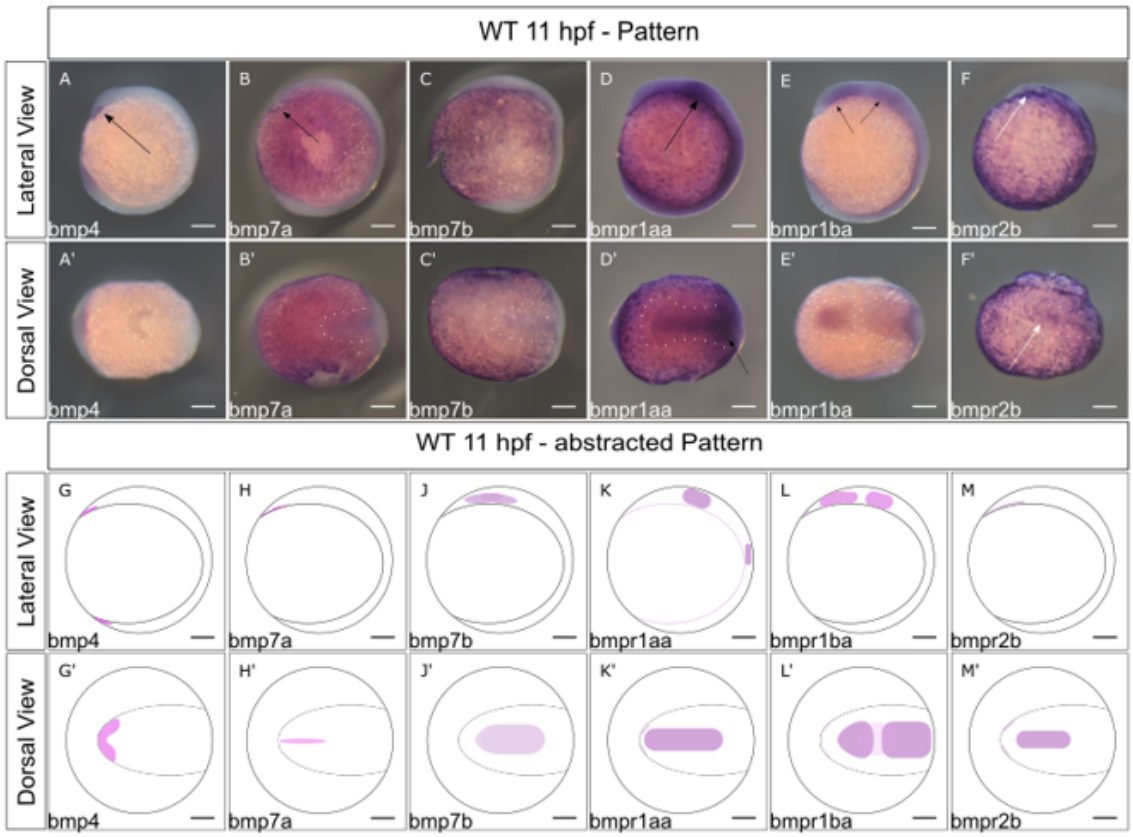

Figure 1

Figure 1: **Expression patterns and domains of bmp ligands and receptors in wildtype at 11 hpf in in lateral and dorsal view.**
A-F' show pictures of exemplary specimen with typical patterns. **G-M'** show schemes of the respective patterns. **A, A', G and G'** show the expression pattern of *bmp4* (4 embryos, 4 with pattern). Note the expression in the most anterior and posterior tip of the embryo. The top view shows a distinct crescent form.**B, B', H and H'** show the expression pattern of *bmp7a* (4 embryos, 4 with pattern). Here, a domain in the prospective head is visible, albeit adherent to the midline. **C, C', J and J'** show the expression domains of *bmp7b* (5 embryos, 4 with pattern). Please note a centralized domain stretching caudally from the prospective head to approximately one fourth of the embryo's length, **D, D', K and K'** show the pattern of *bmpr1aa* (7 embryos, 5 with pattern). A ventral expression domain is visible underlying the embryo, also visible in the top view (D', dotted lines) Arrows mark a prominent domain, in the region of the putative presumptive midbrain hindbrain boundary. **E, E', L and L'** show the expression pattern of *bmpr1ba* (6 embryos, 6 with pattern). Two prominent and separate domains are seen in the prospective head (arrows). The separation of these domains (dotted lines) is clearly seen in the top view. **F, F', M and M'** show the expression pattern of *bmpr2b* (6 embryos, 6 with pattern). Here an underlying expression domain is seen, stretching along the midline of the embryo (arrows).

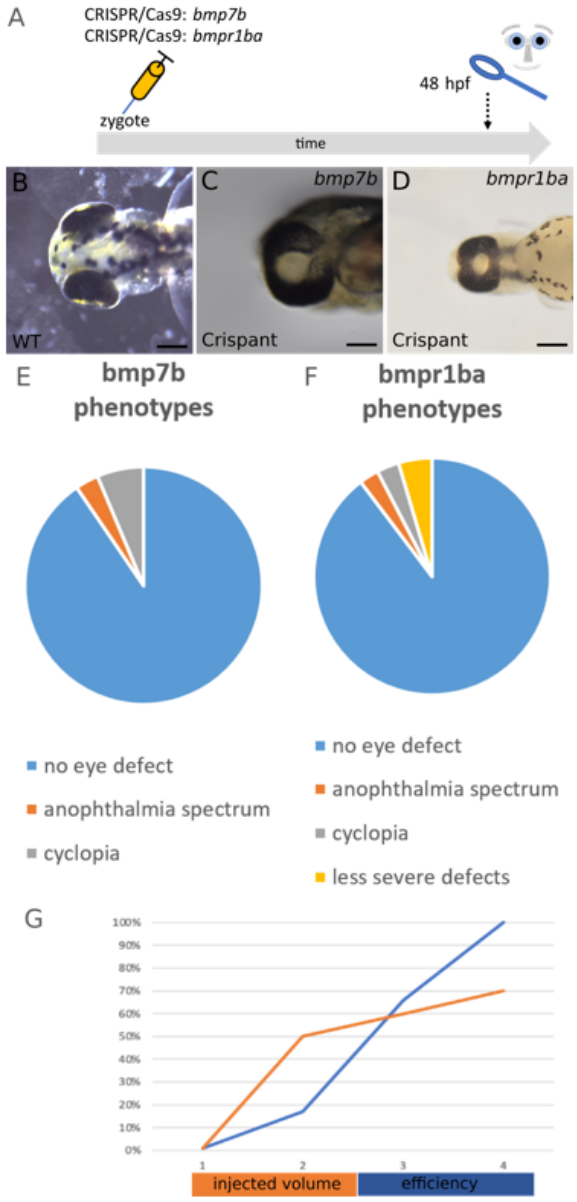

Figure 2

Figure 2: Targeting of *bmp7b* and *bmpr1ba* with CRISPR/Cas9 results in cyclopia.
A: summary of experimental procedure. embryos were injected at 1-cell-stage and analyzed at 48 hpf. **B:** wildtype. dorsal view. **C:** *bmp7b* Crispant with cyclopia. ventral view. **D:** *bmpr1ba* Crispant with cyclopia. ventral view. scalebars indicate 200 µm. **E, F:** comparison of phenotype yield in *bmp7b* and *bmpr1ba* Crispants. **E:** 6% (4 embryos) of *bmp7b* Crispants had cyclopia and 4% displayed phenotypes of the anophthalmia spectrum (1 anophthalmia, 1 one lateral eye). total phenotype yield 10% (8/63). Data from one experiment.
F: 3% (8 embryos) of *bmpr1ba* Crispants had cyclopia, 3% displayed phenotypes of the anophthalmia spectrum (5 anophthalmia, 2 one lateral eye) and 5% had less severe defects (5 microphthalmia, 5 dysmorphic eyes, 2 synophthalmia). total phenotype yield 10% (27/262). Data from 6 separate experiments. **G:** Increase in efficiency by increasing the injected volume of the CRISPR/Cas9 cocktail.

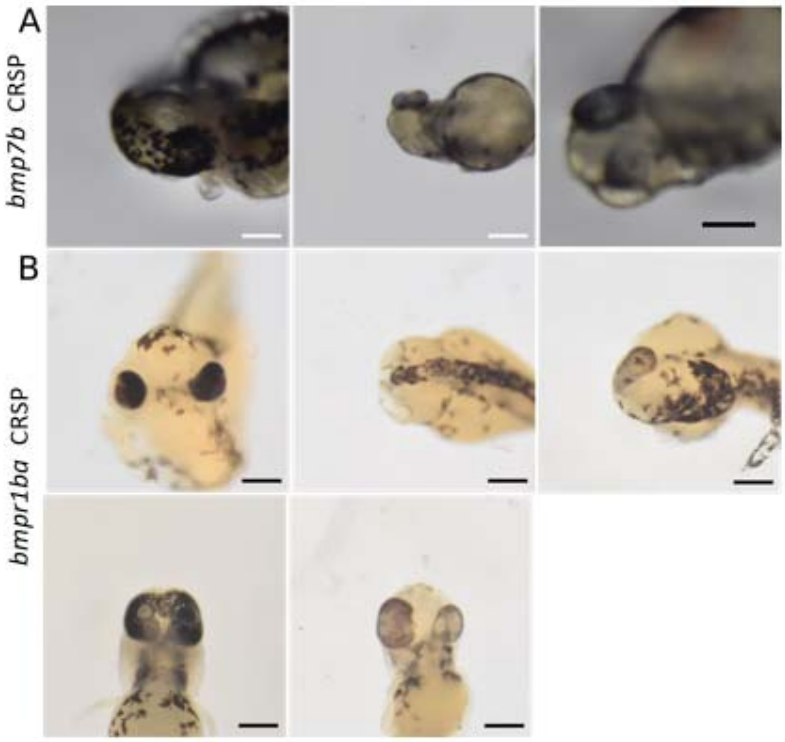

Figure 2 Supplement

Figure 2 Supplement: **Additional phenotypes observed after targeting *bmp7b* and *bmpr1ba* with CRISPR/Cas9.**
A, B: *bmp7b* Crispants, dorsal view. **A:** anophthalmia. **B:** one lateral eye. **C-G**: *bmpr1ba*-Crispants. **C:** microphthalmia. ventral view. **D**: anophthalmia. dorsal view. **E:** one lateral eye. dorsal view. **F:** dysmorphic eyes with ocular hypotelorism. ventral view. **G:** synophthalmia. ventral view. scalebars indicate 200 µm.

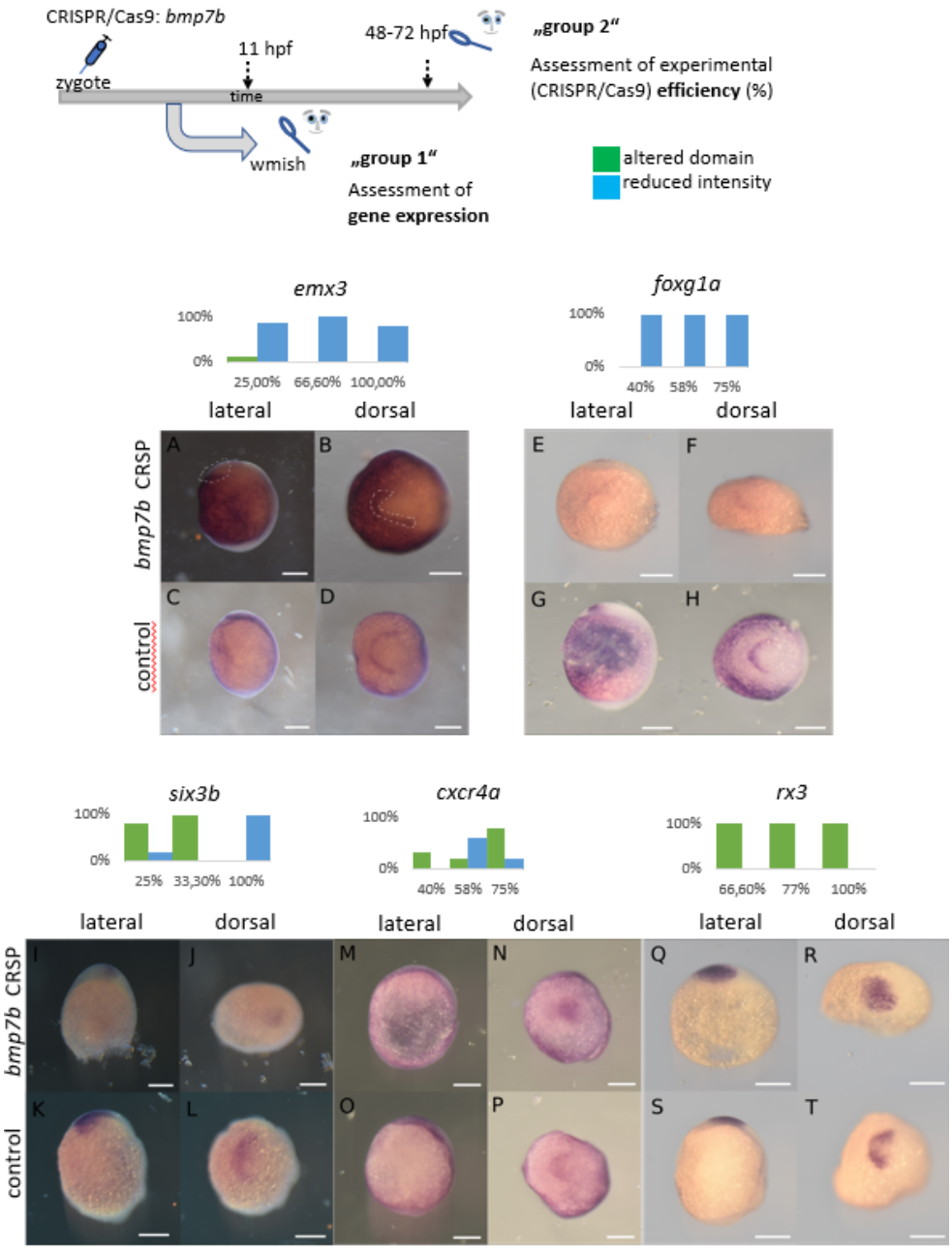

Figure 3

Figure 3: Analysis of gene expression patterns in ANP domains in Crispants for *bmp7b* and controls (I)

Scheme: Experimental procedure: CRISPR/Cas9 injections into zygotes, subsequent separation of embryos: group 1: wmish analysis, group 2: assessment of experimental efficiency (5-6 un-injected embryos served as controls for each experiment)

Overall, individual evaluation of expression patterns is presented in bar charts for the respective genes analyzed. Three experiments were evaluated for each gene. The bars inform about to what extent the expression domain was either altered in form or altered in expression

intensity. Experimental metadata is given in **Table 1**. The respective experimental efficiency is given as a percent value beneath the bars. 100% is considered either phenotype in 100 % of surviving embryos or no survivors. **A-D** show expression patterns of *emx* in controls (**C, D**) and Crispants **(A, B**). Please note the reduction of expression in the lateral domain (right) in **B**. **E-H** show expression of *foxg1a* in controls (**G, H**) and Crispants (**E, F**). Please note the reduction of expression most seen in the lateral domain (right) in **F**. **I-L** show expression of *six3b* in controls (**K, L**) and Crispants (**I, J**). Please note the condensed expression domain closer to the midline (**J)**. **M-P** show expression of *cxcr4a* in controls (**O, P**) and Crispants (**M, N**,). Please note the condensed expression domain closer to the midline (**N)**. **Q-T** show expression of *rx3* in controls (**S, T**) and Crispants (**Q, R**). Please note the condensed expression domain closer to the midline (**R)**.

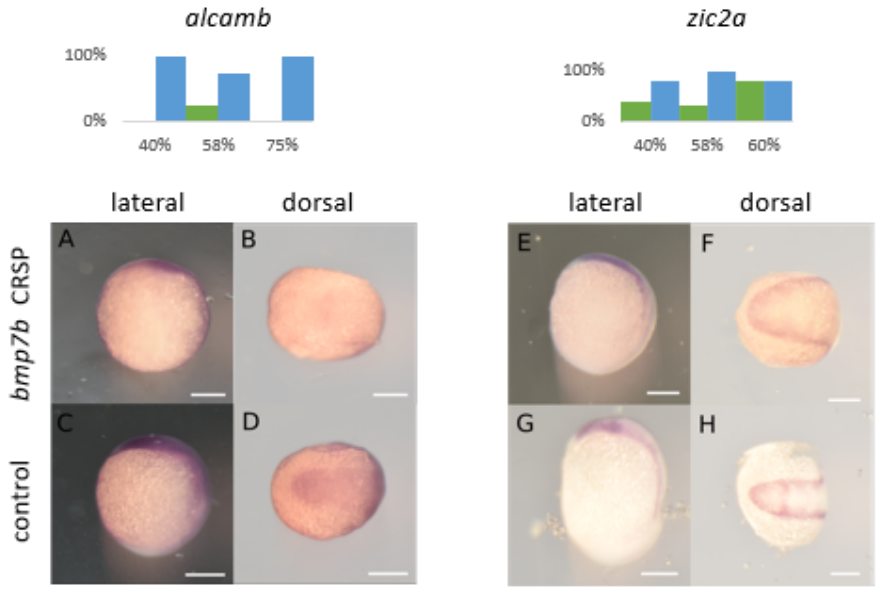

Figure 4

Figure 4: Analysis of gene expression patterns in ANP domains in Crispants for *bmp7b* and controls (II)

Overall, individual evaluation of expression patterns is presented in bar charts for the respective genes analyzed. Three experiments were evaluated for each gene, the respective experimental efficiency is given as a percent value beneath the bars. The bars inform about to what extent the expression domain was either altered in form or altered in expression intensity. Experimental metadata is given in **Table 1**. **A-D** show expression of *alcamb* in controls (**C, D**) and Crispants (**A,B**). Please note the reduced expression (**B)**. **E-H** show expression of *zic2a* in controls (**G, H**) and Crispants (**E, F**). Please note the extended width in between the lateral expression domains as well as the reduced expression at the prospective posterior domain of the ANP (**J**).

Gene of interest	Experiment	No of injected embryos for analysis (wmish)	Experimental efficiency
	1	7	25%
	2	4	100%
emx3	3	5	66,60%
	1	5	40%
	2	3	58,30%
foxg1a	3	4	75%
	1	5	25%
	2	4	100%
six3b	3	4	33,30%
	1	3	40%
	2	5	58%
cxcr4a	3	5	75%
	1	1	100%
	2	3	66,60%
rx3	3	2	77%
	1	4	44%
	2	4	58,30%
alcamb	3	5	75%
	1	5	40%
	2	3	58,30%
zic2a	3	5	60%

Table 1

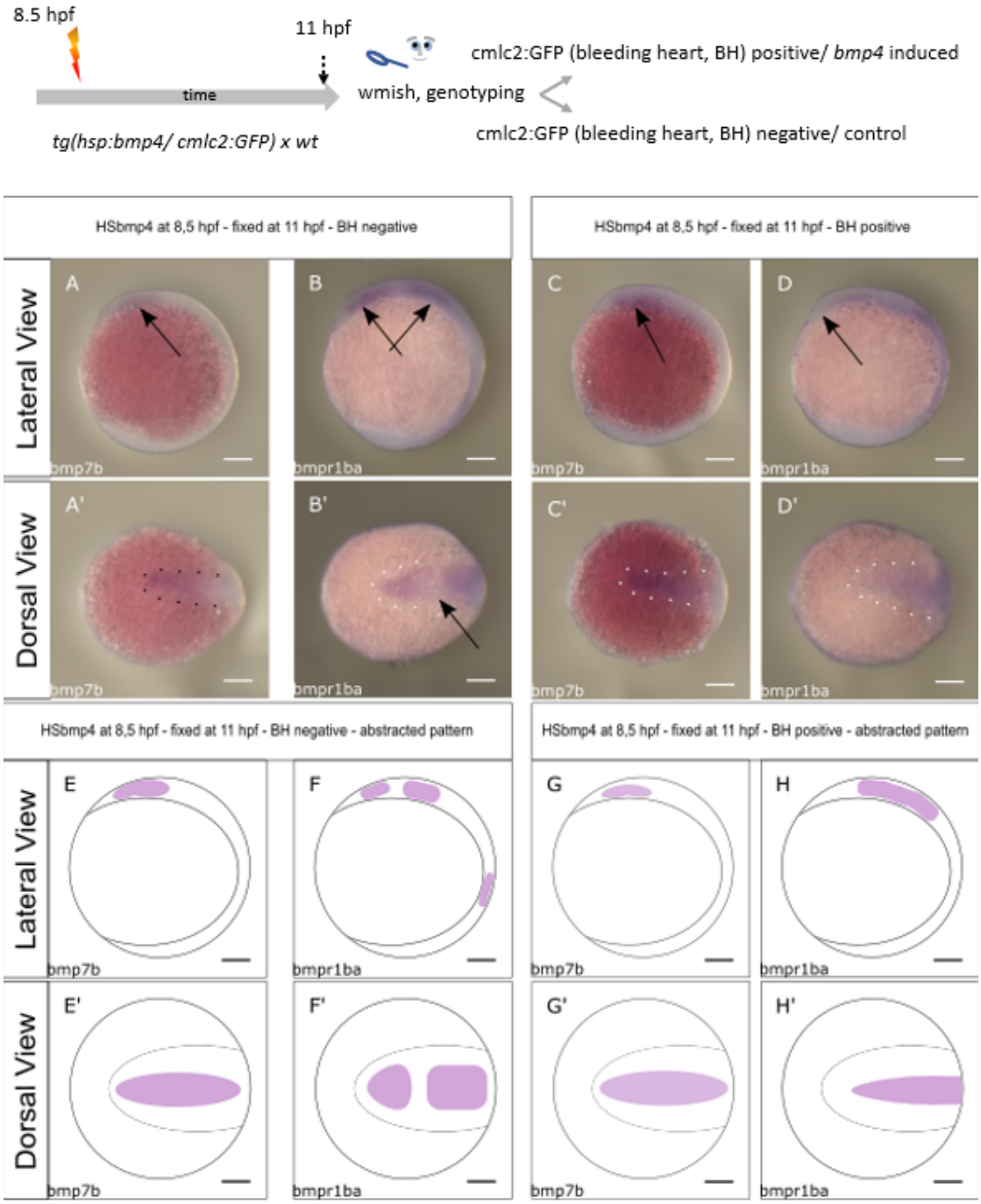

Figure 5

Figure 5:
Expression patterns and domains of *bmp7b* and *bmpr1ba* in specimen after induction of *bmp4* and in controls (lateral and dorsal views)
Scheme: Heat shock of outcrossed transgenes *tg(hsp:bmp4/ cmlc2:GFP)* at 8.5 hpf and fixation for whmish at 11 hpf. Genotyping and separation of recorded expression patterns
A-B' show pictures of exemplary specimen with typical expression patterns, genotyped cmlc2:GFP/ bleeding heart (BH) negative. **C-D'** show pictures of exemplary specimen with

typical expression patterns genotyped cmlc2:GFP/ bleeding heart (BH) positive. **E-H'** show schematic drawing of the patterns respectively. **A, A', E and E'** show the expression pattern of *bmp7b* without *bmp4* induction (3 embryos, 3 embryos with pattern). Note the singular domain in the front of the prospective head. It stretches almost to the dorsal end of the embryo. It is localized along the midline. **B, B', F and F'** show the expression domain of the *bmpr1ba* without *bmp4* induction (5 embryos, 5 embryos with pattern). Here two distinct and separate domains stand out, with the anterior one being localized at the anterior part of the prospective head and the second one being localized further caudally. **C, C'. G and G'** show the expression domain of *bmp7b* after induction of *bmp4* (8 embryos, 6 embryos with pattern). The expression domain remains similar to the uninduced one, albeit with a slight smaller projection dorsally, seen in the lateral perspective (please note the arrow in C).
D, D', H and H' show the expression domain of the *bmpr1ba* after induction of *bmp4* (16 embryos, 16 embryos with pattern). Now a single expression domain is visible that spans continuously from the prospective head caudally. A domain without expression is visible at the anterior end of the embryo (arrow in D).

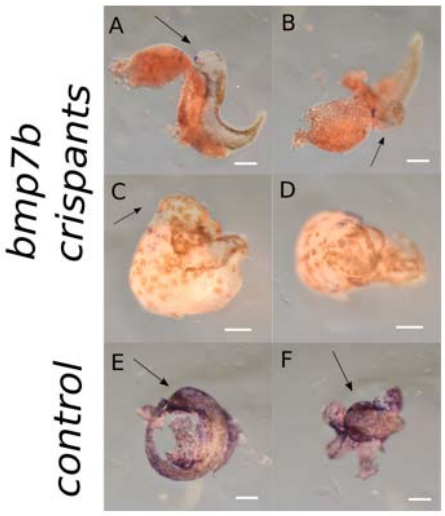

Figure 5 Supplement

Figure 5 Supplement: No crypt-oculoid in *bmp7b* Crispants
A-D: *bmp7b* Crispants, two embryos, dorsal and lateral views, wmish for *rx2*, please note that we do not observe a "crypt oculoid", rather, if at all, a few clusters of expression (arrows), **E, F:** control embryos, *rx2* wmish, scalebars: 400 µm

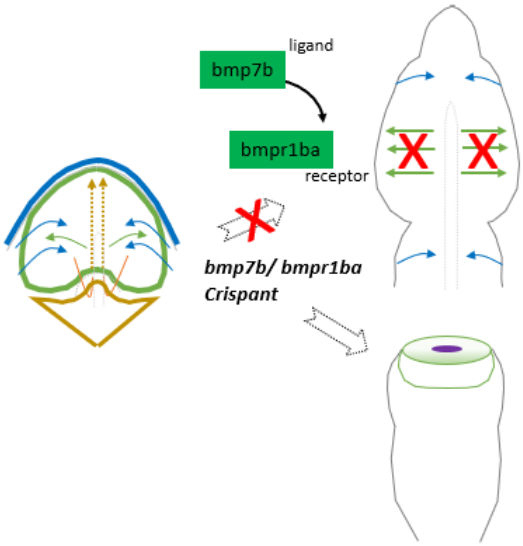

rx3/cxcr4a/six3b	*emx3/foxg1a*	*zic2a*	*rx2* in anophthalmia
condensed expression close to midline	Normal expression domain (reduced level)	extended width between lateral expression domains, reduction of transverse domain in posterior ANP	loss of rx2 in anophthalmic embryos (Figure suppl)

Figure 6 Summary

Figure 6
Schematic and tabular summary of major findings:
In Crispants for *bmp7b* (and *bmpr1ba*) the separation of the eye field fails during early developmentand the development results in cyclopia. Genes expressed in the eye field *rx3*, *cxcr4a* and *six3b* are condensed to the midline in Crispants (shown for *bmp7b*). Genes expressed in the prospective telencephalic domain, *emx3* and *foxg1a*, show an overall normal form of their expression domain (in terms of separation from the midline), however, reduced levels of expression intensity. The lateral expression domains of zic2a were found at an extended width.In cases of Crispants resulting in anophthalmia, no “crypt-oculoid” was found.

References

Addissie, Y. A., Troia, A., Wong, Z. C., Everson, J. L., Kozel, B. A., Muenke, M., Lipinski, R. J., Malecki, K. M. C. and Kruszka, P. (2021). Identifying environmental risk factors and gene-environment interactions in holoprosencephaly. *Birth Defects Res* 113, 63–76.

Alexander, C., Piloto, S., Le Pabic, P. and Schilling, T. F. (2014). Wnt signaling interacts with bmp and edn1 to regulate dorsal-ventral patterning and growth of the craniofacial skeleton. *PLoS Genet* 10, e1004479.

Bachiller, D., Klingensmith, J., Kemp, C., Belo, J. A., Anderson, R. M., May, S. R., McMahon, J. A., McMahon, A. P., Harland, R. M., Rossant, J., et al. (2000). The organizer factors Chordin and Noggin are required for mouse forebrain development. *Nature* 403, 658–661.

Bielen, H. and Houart, C. (2012). BMP signaling protects telencephalic fate by repressing eye identity and its Cxcr4-dependent morphogenesis. *Dev. Cell* 23, 812–822.

Bongiovanni, C., Bueno-Levy, H., Pena, D. P., Bono, I. D., Miano, C., Boriati, S., Pra, S. D., Sacchi, F., Redaelli, S., Bergen, M., et al. (2024). BMP7 promotes cardiomyocyte regeneration in zebrafish and adult mice. *Cell Reports* 43,.

Bulk, J., Kyrychenko, V., Rensinghoff, P. M., Ghaderi Ardekani, Z. and Heermann, S. (2023a). Holoprosencephaly with a Special Form of Anophthalmia Result from Experimental Induction of bmp4, Oversaturating BMP Antagonists in Zebrafish. *Int J Mol Sci* 24, 8052.

Bulk, J., Kyrychenko, V., Rensinghoff, P. M., Ghaderi Ardekani, Z. and Heermann, S. (2023b). Holoprosencephaly with a Special Form of Anophthalmia Result from Experimental Induction of bmp4, Oversaturating BMP Antagonists in Zebrafish. *Int J Mol Sci* 24, 8052.

Dasgupta, S., Cheng, V. and Volz, D. C. (2021). Utilizing zebrafish embryos to reveal disruptions in dorsoventral patterning. *Curr Protoc* 1, e179.

Dong, X.-R., Wan, S.-M., Zhou, J.-J., Nie, C.-H., Chen, Y.-L., Diao, J.-H. and Gao, Z.-X. (2022). Functional Differentiation of BMP7 Genes in Zebrafish: bmp7a for Dorsal-Ventral Pattern and bmp7b for Melanin Synthesis and Eye Development. *Front Cell Dev Biol* 10, 838721.

Dudley, A. T., Lyons, K. M. and Robertson, E. J. (1995). A requirement for bone morphogenetic protein-7 during development of the mammalian kidney and eye. *Genes Dev* 9, 2795–2807.

El-Brolosy, M. A. and Stainier, D. Y. R. (2017). Genetic compensation: A phenomenon in search of mechanisms. *PLoS Genet* 13, e1006780.

El-Brolosy, M. A., Kontarakis, Z., Rossi, A., Kuenne, C., Günther, S., Fukuda, N., Kikhi, K., Boezio, G. L. M., Takacs, C. M., Lai, S.-L., et al. (2019). Genetic compensation triggered by mutant mRNA degradation. *Nature* 568, 193–197.

Gipson, G. R., Goebel, E. J., Hart, K. N., Kappes, E. C., Kattamuri, C., McCoy, J. C. and Thompson, T. B. (2020). Structural perspective of BMP ligands and signaling. *Bone* 140, 115549.

Golden, J. A., Bracilovic, A., McFadden, K. A., Beesley, J. S., Rubenstein, J. L. R. and Grinspan, J. B. (1999). Ectopic bone morphogenetic proteins 5 and 4 in the chicken forebrain lead to cyclopia and holoprosencephaly. *Proc Natl Acad Sci U S A* 96, 2439–2444.

Heermann, S., Schütz, L., Lemke, S., Krieglstein, K. and Wittbrodt, J. (2015). Eye morphogenesis driven by epithelial flow into the optic cup facilitated by modulation of bone morphogenetic protein. *Elife* 4, e05216.

Hua, R., Yu, S., Liu, M. and Li, H. (2018). A PCR-Based Method for RNA Probes and Applications in Neuroscience. *Frontiers in Neuroscience* 12,.

Karsenty, G., Luo, G., Hofmann, C. and Bradley, A. (1996). BMP 7 Is Required for Nephrogenesis, Eye Development, and Skeletal Patterninga. *Annals of the New York Academy of Sciences* 785, 98–107.

Knickmeyer, M. D., Mateo, J. L., Eckert, P., Roussa, E., Rahhal, B., Zuniga, A., Krieglstein, K., Wittbrodt, J. and Heermann, S. (2018a). TGFβ-facilitated optic fissure fusion and the role of bone morphogenetic protein antagonism. *Open Biol* 8,.

Knickmeyer, M. D., Mateo, J. L., Eckert, P., Roussa, E., Rahhal, B., Zuniga, A., Krieglstein, K., Wittbrodt, J. and Heermann, S. (2018b). TGFβ-facilitated optic fissure fusion and the role of bone morphogenetic protein antagonism. *Open Biol* 8, 170134.

Knickmeyer, M. D., Mateo, J. L. and Heermann, S. (2021). BMP Signaling Interferes with Optic Chiasm Formation and Retinal Ganglion Cell Pathfinding in Zebrafish. *Int J Mol Sci* 22, 4560.

Little, S. C. and Mullins, M. C. (2004). Twisted gastrulation promotes BMP signaling in zebrafish dorsal-ventral axial patterning. *Development* 131, 5825–5835.

Luo, G., Hofmann, C., Bronckers, A. L., Sohocki, M., Bradley, A. and Karsenty, G. (1995). BMP-7 is an inducer of nephrogenesis, and is also required for eye development and skeletal patterning. *Genes Dev.* 9, 2808–2820.

Matsunaga, E. and Shiota, K. (1977). Holoprosencephaly in human embryos: epidemiologic studies of 150 cases. *Teratology* 16, 261–272.

Morcillo, J., Martínez-Morales, J. R., Trousse, F., Fermin, Y., Sowden, J. C. and Bovolenta, P. (2006). Proper patterning of the optic fissure requires the sequential activity of BMP7 and SHH. *Development* 133, 3179–3190.

Pineda-Alvarez, D. E., Solomon, B. D., Roessler, E., Balog, J. Z., Hadley, D. W., Zein, W. M., Hadsall, C. K., Brooks, B. P. and Muenke, M. (2011). A broad range of ophthalmologic anomalies is part of the holoprosencephaly spectrum. *Am J Med Genet A* 155A, 2713–2720.

Pomreinke, A. P., Soh, G. H., Rogers, K. W., Bergmann, J. K., Bläßle, A. J. and Müller, P. (2017). Dynamics of BMP signaling and distribution during zebrafish dorsal-ventral patterning. *eLife* 6, e25861.

Quiring, R., Wittbrodt, B., Henrich, T., Ramialison, M., Burgtorf, C., Lehrach, H. and Wittbrodt, J. (2004). Large-scale expression screening by automated whole-mount in situ hybridization. *Mech. Dev.* 121, 971–976.

Shawi, M. and Serluca, F. C. (2008). Identification of a BMP7 homolog in zebrafish expressed in developing organ systems. *Gene Expr. Patterns* 8, 369–375.

Stemmer, M., Thumberger, T., del Sol Keyer, M., Wittbrodt, J. and Mateo, J. L. (2015). CCTop: An Intuitive, Flexible and Reliable CRISPR/Cas9 Target Prediction Tool. *PLoS ONE* 10, e0124633.

Tekendo-Ngongang, C., Muenke, M. and Kruszka, P. (1993). Holoprosencephaly Overview. In *GeneReviews®* (ed. Adam, M. P.), Feldman, J.), Mirzaa, G. M.), Pagon, R. A.), Wallace, S. E.), Bean, L. J.), Gripp, K. W.), and Amemiya, A.), p. Seattle (WA): University of Washington, Seattle.

Thawani, A. and Groves, A. K. (2020). Building the Border: Development of the Chordate Neural Plate Border Region and Its Derivatives. *Frontiers in Physiology* 11,.

Thumberger, T., Tavhelidse-Suck, T., Gutierrez-Triana, J. A., Cornean, A., Medert, R., Welz, B., Freichel, M. and Wittbrodt, J. (2022). Boosting targeted genome editing using the hei-tag. *Elife* 11, e70558.

Wawersik, S., Purcell, P., Rauchman, M., Dudley, A. T., Robertson, E. J. and Maas, R. (1999a). BMP7 acts in murine lens placode development. *Dev Biol* 207, 176–188.

Wawersik, S., Purcell, P., Rauchman, M., Dudley, A. T., Robertson, E. J. and Maas, R. (1999b). BMP7 acts in murine lens placode development. *Dev Biol* 207, 176–188.

Willot, V., Mathieu, J., Lu, Y., Schmid, B., Sidi, S., Yan, Y.-L., Postlethwait, J. H., Mullins, M., Rosa, F. and Peyriéras, N. (2002). Cooperative Action of ADMP- and BMP-Mediated Pathways in Regulating Cell Fates in the Zebrafish Gastrula. *Developmental Biology* 241, 59–78.

Wilson, S. I. and Edlund, T. (2001). Neural induction: toward a unifying mechanism. *Nat Neurosci* 4 Suppl, 1161–1168.

Wu, R. S., Lam, I. I., Clay, H., Duong, D. N., Deo, R. C. and Coughlin, S. R. (2018). A Rapid Method for Directed Gene Knockout for Screening in G0 Zebrafish. *Dev Cell* 46, 112-125.e4.